

Reconstruction of Computer Generated Holograms by Spatial Light Modulators

M. Kovachev¹, R. Ilieva¹, L. Onural¹, G.B. Esmer¹, T. Reyhan¹, P. Benzie²,
J. Watson², and E. Mitev³

¹Dept. of Electrical and Electronics Eng., Bilkent University, TR-06800 Ankara, Turkey

²University of Aberdeen, King's College, AB24 3FX, Scotland, UK

³Bulgarian Institute of Metrology, Sofia, Bulgaria

Abstract. Computer generated holograms generated by using three different numerical techniques are reconstructed optically by spatial light modulators. Liquid crystal spatial light modulators (SLM) on transmission and on reflection modes with different resolutions were investigated. A good match between numerical simulation and optically reconstructed holograms on both SLMs was observed. The resolution of the optically reconstructed images was comparable to the resolution of the SLMs.

1 Introduction

Computer generated holograms (CGHs) are one possible technique for 3D (3-dimensional) imaging. In holography the *a priori* information of a 3D object is stored as an interference pattern. A hologram contains high spatial frequencies. Various methods, such as compression of fringe patterns, generation of horizontal-parallax-only (HPO) holograms and computation of binary holograms, have been proposed to reduce the bandwidth requirements. A spatial light modulator (SLM) with high resolution and a small pixel pitch is required to optically reconstruct a dynamic CGH. For a good match between the recorded object wavefront and the reconstructed wavefront, it is necessary to generate holograms suitable to the SLMs parameters (for instance pixel pitch, pixel count, pixel geometry) and reconstruction wavelength. SLMs may be electronically written by CGHs or holograms captured directly from a digital camera. Recently, digital holography has seen renewed interest, with the development of mega pixel (MP) SLMs as well as MP charge-coupled devices (CCDs) with high spatial resolution and dynamic range.

2 Backgrounds

Spatial Light Modulator can be used as a diffractive device to reconstruct 3D images from CGHs computed using various techniques like Rayleigh-Sommerfeld diffraction, Fresnel-Kirchhoff integral, Fresnel (near field) or Fraunhofer (far field) approximations[10-16]. For successful reconstruction, the size of the SLM, reconstruction wavelength, the distance between the SLM and the image location and

many other parameters must be carefully considered. Three methods for CGH are considered in this paper. The generation of CGH is computationally expensive, therefore a number of algorithms have been employed to exploit redundancy and reduce computation time [6]. Lucente *et al.* utilised a bipolar intensity method, described herein, to reduce the computation time of CGH generation [7]. Ito *et al.* further applied this method to reconstruction of CGH holograms onto liquid crystal on silicon (LCoS) spatial light modulators [8,9].

Predominantly in-line holograms are reconstructed with LCoS SLMs. The advantage of the in-line reconstruction geometry is that the reference beam and object beam are collinear, thus the resolution requirements of the SLM are less demanding [10].

The bipolar intensity method derives its name from producing an interference pattern centered about zero, whose intensity is dependant upon the cosinusoidal term in Eq.1. Each pixel location (x_α, y_α) of the SLM can be defined, where, $x_j, y_j, z_j,$ are the real co-ordinate location of the points on an object and a_j is the amplitude of each point on the object, dependant upon the radial distance from each object point.

$$I_{bipolar}(x_\alpha, y_\alpha) = \sum_{j=1}^{No.pts.} A_j \cos\left(\frac{2\pi}{\lambda} \sqrt{(x_\alpha - x_j)^2 + (y_\alpha - y_j)^2 + z_j^2}\right). \quad (1)$$

On calculation of 1 it is necessary to normalise the bipolar intensity so that all values are positive and can be addressed to the spatial light modulator. This is easily be down by adding a dc offset to all pixels. The dynamic range of the intensity levels are then assigned to 8 bit intensity levels, which can be directly used to address the SLM. Eq.1 enables the reconstruction of three dimensional scenes described as object points and can be easily implemented into graphics commodity hardware for fast real-time computation of holograms [11].

Two other methods for hologram computer generation use wavefront propagation theory. One of them uses Fresnel diffraction and the other one uses Rayleigh-Sommerfeld diffraction.

In the case of Fresnel diffraction the first step is to calculate the wavefront propagation from the object $U(x,y,0)$ at a distance z to the hologram plane. The field in the hologram plane $U(x',y',z)$ according to Fresnel diffraction theory is [1]:

$$U(x', y', z) = \frac{e^{jkz}}{j\lambda z} \iint U(x, y, 0) \exp\left\{j \frac{k}{2z} [(x'-x)^2 + (y'-y)^2]\right\} dx dy \quad (2)$$

Eq.2 is convolution of the object $U(x,y,0)$ and a kernel $K(x-x',y-y',z)$ given by,

$$K(x-x', y-y', z) = -\frac{j}{\lambda z} \exp(jkz) \exp\left[jk \frac{(x-x')^2}{2z}\right] \exp\left[jk \frac{(y-y')^2}{2z}\right]. \quad (3)$$

For a moment we shall drop the constant terms for simplicity, and denote $U(x, y) = U(x, y, 0)$. Now if we have some discrete structure, on which the complex input field is defined (e.g. SLM), with dimensions $X \times Y$ for the inner integral, with respect to $x,$ we can write

$$\int_{-X/2}^{+X/2} U(x, y) \exp\left[jk \frac{(x-x')^2}{2z}\right] dx = \int_{x_1}^{x_2} B dx + \int_{x_2}^{x_3} B dx + \int_{x_3}^{x_4} B dx + \dots, \text{ where,} \quad (4)$$

$$B = U(x, y) \exp\left[jk \frac{(x-x')^2}{2z}\right], \quad U(x, y) = \text{const} = U(x_i, y); \text{ for } \begin{cases} x_i \leq x \leq x_{i+1} \\ y = \text{const} \end{cases}$$

Thus we split the original integral into many integrals each defined over a single pixel and set the integral boundaries to coincide with pixel boundaries. Over the area of a single pixel, the input field is constant and it can be moved out of the integral:

$$\int_{x_i}^{x_{i+1}} B dx = U(x_i, y) \int_{x_i}^{x_{i+1}} \exp\left[jk \frac{(x-x')^2}{2z}\right] dx$$

For the exponent argument and integral boundaries the following substitutions can be made: $(x-x')\sqrt{2}/\sqrt{\lambda z} = \tau$; $dx = \sqrt{\lambda z}/\sqrt{2} d\tau$; $\tau|_{x=x_i} = \tau_i$; and each of the integrals in (4) is explained in terms of Fresnel's integrals as:

$$\int_{\tau_i}^{\tau_{i+1}} \exp\left(\frac{j\pi}{2}\tau^2\right) d\tau = \int_0^{\tau_{i+1}} (\dots) - \int_0^{\tau_i} (\dots) = C(\tau_{i+1}) + jS(\tau_{i+1}) - C(\tau_i) - jS(\tau_i),$$

where $C(\tau_i)$ and $S(\tau_i)$ are Cosine and Sine Fresnel integrals. Integrals along the y direction can be calculated in the same way. After several generalizations the following expression for both directions was derived:

$$U(x'_j, y'_l) = -\frac{1}{2} \sum_{k=1}^M \sum_{i=1}^N U(x_i, y_k) \{ [jC(\tau_{(i+1)-j}) + S(\tau_{(i+1)-j}) - jC(\tau_{i-j}) - S(\tau_{i-j})] \cdot [jC(\tau_{(k+1)-l}) + S(\tau_{(k+1)-l}) - jC(\tau_{k-l}) - S(\tau_{k-l})] \}, \quad (5)$$

which is a 2D discrete convolution. The kernel, expressed with the terms in brackets {}, can be easily calculated by using standard algorithms. The convolution can be calculated directly or by discrete Fourier transform.

The second step in calculation of a CGH is to add in a collinear - for inline hologram, or slanted - for off-axis hologram, reference beam.

Rayleigh-Sommerfeld diffraction method is described below. In the simulations, the distance parameter r is chosen as $r \gg \lambda$. Moreover, we are not dealing the evanescent wave components. Under these constraints, Rayleigh-Sommerfeld diffraction integral and plane wave decomposition become equal to each other [14, 15]. The diffraction field relationship between the input and output fields by utilizing the plane wave decomposition is shown as

$$U(x', y', z) = \int_{-2\pi/\lambda}^{2\pi/\lambda} \int_{-2\pi/\lambda}^{2\pi/\lambda} \mathfrak{S}[U(x, y, 0)] \exp[j(k_x x + k_y y)] \exp(k_z z) dk_x dk_y, \quad (6)$$

where \mathfrak{S} is the Fourier transform (FT). The terms k_x , k_y and k_z are the spatial frequencies of the propagating waves along the x , y and z axes. Also, the variable k_z can be computed by the variables k_x and k_y , as a result of dealing with monochromatic

light propagation. The relationship can be given as $k_z = \sqrt{k^2 - k_x^2 - k_y^2}$, where $k=2\pi/\lambda$. The expression in Eq.6 can be rewritten as:

$$U(x', y', z) = \mathfrak{F}^{-1}\{\mathfrak{F}[U(x, y, 0)]\exp(j\sqrt{k^2 - k_x^2 - k_y^2}z)\},$$

where \mathfrak{F}^{-1} is the inverse FT. We deal with propagating waves, hence the diffraction field is bandlimited. Moreover, to have finite number of plane waves in the calculations, we work with periodic diffraction patterns. To obtain the discrete representation, Eq.6 is sampled uniformly along the spatial axes with $x=nX_s$, $y=mX_s$ and $z=pX_s$, where X_s is the sampling period. Moreover, uniform sampling is applied on the frequency domain with $k_x=2\pi n'/NX_s$ and $k_y=2\pi m'/NX_s$. The resultant discrete form of the plane wave decomposition approach is

$$U_D(n, m, p) = DFT^{-1}\{DFT[U_D(n, m, 0)]H_p(n', m')\} \tag{7}$$

where term

$H_p(n', m') = \exp(j2\pi\sqrt{\beta^2 - n'^2 - m'^2} p / N)$ and $\beta=NX_s/\lambda$. The discrete diffraction field $U_D(n, m, p)$ is:

$$U_D(n, m, p) = U(nX_s, mX_s, pX_s)$$

In order to physically reconstruct CGHs by the described methods a LC or LC on Silicon (LCoS) SLM can be employed [12, 13]. Due to the limited spatial bandwidth product offered by the SLM, it is only possible to reconstruct CGH holograms with a limited viewing angle and spatial resolution.

3 Computer Simulations

A program for computation of forward and backward wavefront propagation and CGHs is created using the Fresnel diffraction integral (Eq.5.) It can directly calculate the reconstructed wavefront (object) from the propagated forward complex (amplitude and phase) field without generating a hologram. By applying a reference beam to the forward propagated wavefront a CGH is generated. In our case the CGH reconstruction is obtained using a beam complex conjugated to the reference beam and backward propagated. If a copy of the reference beam is used then the virtual image is reconstructed.

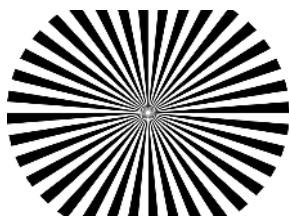


Fig. 1. Object

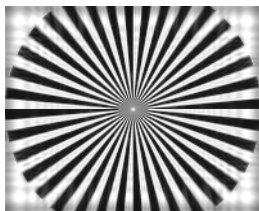


Fig. 2. Computer reconstructed Image

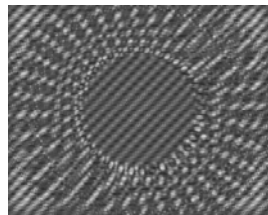


Fig. 3. Off-axis CGH

A star target (Fig.1) was used to test the resolution we could obtain in the image from reconstructed holograms by computer simulation and by the SLM. In Fig. 2 computer reconstructed image is shown. It is calculated from the complex field obtained by propagation of the object wavefront to a distance of 800 mm and back propagating by the same distance. It is seen that the resolution is near to the object resolution. Irregularities in the background (Fig.2) are due to the loss of energy because of the limited SLM size. The diffracted field from the object at 800 mm is about two times larger than the SLM size in x and y directions. In Fig.3 is shown off-axis CGH at an angle of 0.758° .

4 Experimental Results of Reconstructed CGH by SLM

The experimental setup in Fig.4 is used to reconstruct the holograms by LC SLM.(left) and LCoS SLM (right).

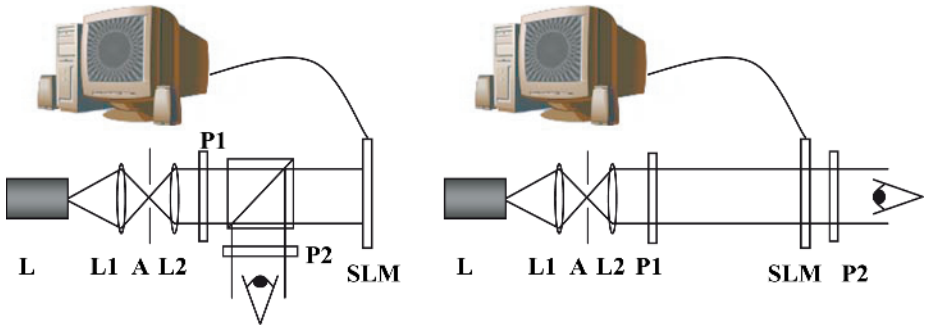


Fig. 4. Reconstruction of an amplitude hologram on a reflective SLM (left) and transmissive SLM (right): L, laser, L1, positive lens, L2, collimating lens, A, aperture, P, polarizer, BS, beam splitter, SLM, spatial light modulator connected to computer via DVI port, P2, analyzer

The combination of lens, L1 and aperture, A, together form a spatial filter arrangement to improve the beam quality and L2 is used to adjust the collimation of the illuminating source (Fig.4). A 635 nm, red laser diode is used with the transmissive LC SLM 17.78 mm diagonal, pixel pitch $12.1 \times 12.1 \mu\text{m}$, resolution 1280×720 . A 633 nm, HeNe is used with the reflective LCoS SLM, pixel pitch $8.1 \times 8.1 \mu\text{m}$, resolution 1900×1200 . Therefore there is a negligible difference in wavelength between optical geometries. The experimental results are shown from pictures taken by a digital camera.

The maximum diffraction angle for a LC SLM is 1.51° and the minimum distance for a Gabor (inline) hologram, to avoid overlapping of diffractive orders in the reconstructed image is 350 mm. The maximum diffraction angle for LCoS SLM is 2.24° .

A reconstructed magnified real image of the star target (Fig.1) from a Fresnel diagonal off-axis CGH (Fig.3, Eq.5) is shown in Fig. 5a. The same hologram, reconstructed by LCoS SLM, is shown in Fig. 5b. Real (upper) and virtual (lower)

images and zero order (middle) are seen therein. An image, reconstructed by LC SLM from inline CGH by Rayleigh -Sommerfeld method (Eq.7) is shown in Fig. 5c. For comparison a sinusoidal wave was used as an object for inline CGH. This was reconstructed by bipolar intensity method (Eq.1) on the LC SLM (Fig.5d) and LCoS SLM (Fig.5e).

It is seen that the resolution of a simulated (Fig.2) and experimentally reconstructed (Fig.5a) Star Target images are almost the same. The quality of reconstructed images by LC SLM and reflective SLM are also comparable.

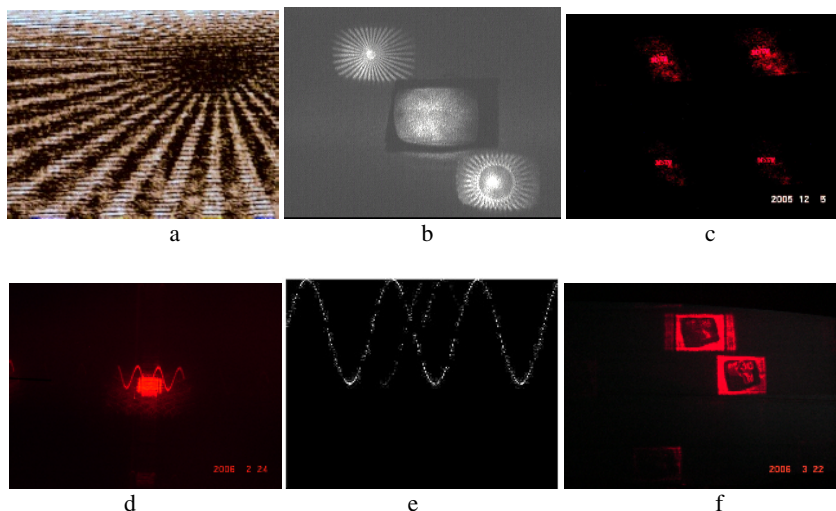


Fig. 5. Reconstructed images by LC and LCoS SLMs

Using the Red, Blue and Green components color holograms can be successfully reconstructed [4,5].

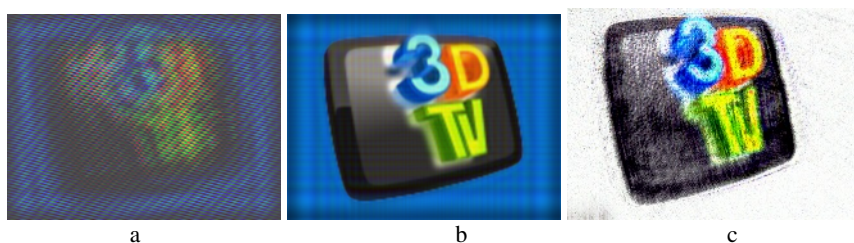


Fig. 6. Color off-axis CGH of 3DTV Logo as an object and reconstructed images

Fig. 6 shows images of off-axis color Fresnel hologram of the planar 3DTV Logo (object) and the reconstructed images from this hologram. The object is split into R,G and B components and separate holograms are computed for each component using Eq.5. The color hologram in Figure 6a is created by superposing the calculated

holograms for the R,G and B components, using their respective colors during the superposition. The reconstruction of the hologram corresponding to the R component by the LC SLM using a red laser is shown in Fig.6c; the picture is captured by a digital camera. Similar SLM reconstructions are carried out also for the G and B holograms and each reconstruction is captured by a digital camera. The captured pictures of the separate SLM reconstructions for each color component are then combined, again digitally, to yield the color picture shown in Fig.6d. Digital reconstructions, instead of SLM reconstructions, are also carried out for comparison, and the result is shown in Fig.6b.

5 Conclusions

The resolution of the experimentally reconstructed images is near to the resolution of images reconstructed by computer simulation. Speckle noise, which further decreases the visual image quality, exists in the experimentally reconstructed images. The diffraction angle from the SLM pixels is very small (only about $1,5^\circ$). This makes it impossible to observe a volume image directly without additional optics.

It is found that for the transmissive and reflective LC SLM set-up, experimentally reconstructed images of Fresnel holograms have resolution near to that of the numerically reconstructed simulations. The specifications of the two SLMs used in experiments were different with respect to pixel pitch, however, this was easily resolved by compensating with the reconstruction distance or adjusting the CGH algorithm accordingly. A beam splitter is required when working with a reflective LC SLM, this acts of as an aperture limiting the viewing angle of the display and complicates the geometry, furthermore additional reflections from surfaces of the beam splitter are disturbing to the reconstruction. In this respect the transmissive LC SLM is more convenient for optical reconstruction of holograms.

Each one of the algorithms described has their relative merits for three-dimensional reconstruction of holographic images. The main advantage of the bipolar intensity method is its ease of implementation by computer graphics cards. Furthermore, it does not a fast Fourier transform implemented on. With this method the reconstruction time scales linearly with the number of data points. An obvious disadvantage of the bipolar intensity method is that an amplitude hologram is required for reconstruction, rather than the often more preferable phase hologram. Primarily a phase hologram, as could be produced by the Fresnel diffraction, is advantageous because less polarizing optics are required, and that increases the quality of the reconstruction.

The Rayleigh-Sommerfeld diffraction integral is a general solution for the diffraction since it does not need Fresnel or Fraunhofer approximations.

Acknowledgement

This work is supported by EC within FP6 under Grant 511568 with the acronym 3DTV.

References

1. Goodman J.W. "Introduction to Fourier Optics" Roberts & Company publisher, US, 3rd edition, 2004.
2. Max Born, Emil Wolf, "Principles of Optics", IV edition, 1968.
3. Gleb Vdovin, "LightPipes: beam propagation toolbox" OKO Technologies, The Netherlands, 1999.
4. Anand Asundi and Vijay Raj Singh, "Sectioning of amplitude images in digital holography", *Meas. Sci. Technol.* 17 (2006) 75–78.
5. Ho Hyung Suh, Color-image generation by use of binary-phase holograms, *Opt. Letters*, Vol. 24, No. 10, (1999), p.661.
6. Lucente M., Computational holographic bandwidth reduction compression, *IBM SYSTEMS JOURNAL*, 35 (3&4), (1996)
7. Lucente M, Interactive computation of holograms using a look-up table, *Journal of Electronic Imaging*, 2 (1), 1993, pp. 28 -34
8. Ito T, Okano K, Color electroholography by three colored reference lights simultaneously incident upon one hologram panel, *Optics Express*, 12 (18), pp. 4320-4325, 2004
9. Ito T, Holographic reconstruction with a 10-um pixel-pitch reflective liquid-crystal display by use of a light-emitting diode reference light, *Optics Express*, 27 (2002)
10. Kries T., Hologram reconstruction using a digital micromirror device, *Opt. Eng.*, 40(6), 926-933, (2001)
11. T. Ito, N. Masuda, K. Yoshimura, A. Shiraki, T. Shimobaba, and T. Sugie, "Special-purpose computer HORN-5 for a real-time electroholography," *Opt. Express* 13, 1923-1932 (2005)
12. Shimobaba T, A color holographic reconstruction system by time division multiplexing with reference lights of laser, *Optical Review*, 10, 2003
13. M. Sutkowski and M. Kujawinski, Application of liquid crystal (LC) devices for optoelectronic reconstruction of digitally store holograms", *Opt. Laser Eng.* 33, 191-201 (2000)
14. G. C. Sherman, "Application of the convolution theorem to Rayleigh's integral formulas," *J. Opt. Soc. Am.*, vol. 57, pp. 546–547, 1967.
15. E. Lalor, "Conditions for the validity of the angular spectrum of plane waves," *J. Opt. Soc. Am.*, vol. 58, pp. 1235–1237, 1968.